Proceedings of the 11th International Conference on Manufacturing Research (ICMR2013), Cranfield University, UK, 19th – 20th September 2013, pp 251-256

EXPERIMENTAL AND NUMERICAL STUDY ON SCRATCHING TEST

Tahsin Tecelli Öpöz
General Engineering Research Institute
Liverpool John Moores University
Liverpool, L8 2TJ, UK
t.t.opoz@ljmu.ac.uk

Xun Chen
General Engineering Research Institute
Liverpool John Moores University
Liverpool, L8 2TJ, UK
x.chen@ljmu.ac.uk

ABSTRACT

This paper presents recent investigation of the material removal mechanism in single grit grinding test. Single grit scratches were generated experimentally by using CBN grit on En24T steel and compared with numerical simulation by using finite element modelling (FEM). The material removal mechanism was observed along the scratch length to understand the effectiveness of ploughing and cutting mechanism throughout the scratch. Experiments showed that cutting is efficient at first half of the scratch while ploughing is significantly higher at the second half of the scratch. At the exit side of the scratch almost no material removal takes place. It has demonstrated that FEM simulations match well with experimental results.

Keywords: single grit scratch, ploughing, cutting.

1 INTRODUCTION

Grinding is a material removal process which is widely used in manufacturing industry as a final finishing process. In order to predict and optimise grinding performance, grinding experiments with the support of computer modelling and simulation become increasingly important. The surface generation in grinding is considered as a result of numerous scratches by irregularly shaped abrasive grits which are bonded together forming a grinding wheel. While a grinding wheel consists of numerous of bonded abrasive grits, a single abrasive grit interaction with workpiece can be considered as the most fundamental element in grinding process. Material removal mechanism with the consideration of grit-workpiece interaction was first put forth by Hahn (1962). He proposed that the material removal in grinding consists of three phases which are rubbing, ploughing and cutting. Rubbing occurs at the initial stage of grit-workpiece interaction at very small region including only elastic deformation in the workpiece, while ploughing phase begins with increasing penetration of the grit into workpiece where the material deformation is in both elastic and plastic regions. With increasing of shearing stress at the ploughed material ahead of the grit, material could not withstand without tearing of material in the form of chip removal, and this is called the cutting phase. Rubbing has negligible contribution to material removal, while ploughing play a crucial role in grinding surface creation and energy consumption (Rowe *et al*. 1997). Rubbing and ploughing are undesired mechanism and should be minimised to improve the grinding performance (Ghosh *et al*. 2008). Most researches of grinding material removal were conducted with shaped tools such as diamond indenter, spherical tool, or negative raked cutting tool to simplify the grit shape effect. As a result, scratching with shaped tools gives better agreement with numerical solution such as finite element simulations (Doman *et al*. 2009, Anderson *et al*. 2011), because the modelling is relatively simple. Most researches on scratching focus on the profile of cross section of the cutting path, few investigation has made along the cutting direction.

One of the earliest scratch test was performed by Takenaka (1966) who observed that chip was produced even at small depth of cut (lower than 0.5 μm) in the form of torn leaves from the workpiece surface although rubbing and ploughing phase are prominent in that range of depth cuts. Material removal was found mainly by cutting process when the depth of cut is higher than 1 μm. Komonduri

(1971) investigated the grinding mechanism by using highly negative rake angled diamond tool and observed chip formation up to rake angle of -75º. König *et al.* (1985) investigated that wear types occur on the abrasive grit during the scratching of carbon steel in different heat treatment conditions (annealed, normalized, hardened). It was found that the wear rate is the highest during annealed condition and the lowest during hardened condition. Wang et al (2001) performed single grit scratching test with a conical diamond tool on pure titanium to characterize the material removal mechanism. Focusing material behaviours, they observed that there exist four zones, namely, a stagnant zone, a lamella zone with shear bands, a hardened sublayer zone, and a propagating zone during front ridge development in scratching test.

Klocke *et al.* (2002) developed a 2D FEM model by using Deform software to simulate the single grit cutting process where the grit is passing through the workpiece material. Doman *et al.* (2009) investigated the rubbing and ploughing stages of single grit grinding by using 3D finite element model performed in LS-DYNA software. In the FEM model, the size of the mesh element at the grit-workpiece contact zone was around 10 µm. Only rubbing and ploughing stages during single grit grinding were investigated. Depth of cut for the simulation ranged from 1 µm to 20 µm. The rubbing to ploughing transition was observed at a depth of cut around 3 µm in the simulation, although in the real tests ploughing was observed at lower depth level. The experimental verification was performed by using an alumina sphere indenter with a diameter of 2 mm. Simulation and experimental results demonstrated a good agreement for force prediction. Anderson *et al*. (2011) investigated the single abrasive grain mechanism by experiment and FEM simulation. Unlike previous work, they used a combined Eulerian and Lagrangian formulation for the FEM model. The 3D FEM model was performed in LS-DYNA hydrocode using explicit time integration. Simulation with a spherical tool only demonstrated ploughing material in front and side of the tool, whereas, a flat nose cutting tool (similar to negative rake angle cutting) produced chips at 4 µm depth of cut. Transition from rubbing to ploughing was not captured, and it was concluded that the three phases of material removal (rubbing, ploughing, and cutting) during abrasive grain cutting seems to occur simultaneously but in different proportion depending on the machining (or simulation) conditions. According to these results, normal forces increased with cutting speed due to strain rate hardening of the workpiece, and tangential forces decreased with cutting speed due to reduction in the coefficient of friction between cutting tool and workpiece.

2 EXPERIMENTAL TEST SETUP

Single grit scratching test was performed on Nanoform250 UltraGrind machine centre. A test setup, shown in Figure 1-(a), was designed and manufactured to accommodate single grit grinding tests. A Kistler 3 axis piezoelectric force sensor was mounted under workpiece to measure forces during single grit scratching. An acoustic emission (AE) sensor was mounted near the workpiece to detect the contact between grit and workpiece. A CBN grit of 40/50 mesh size was used for the scratching test. En24T steel with hardness of 289.2 HV at 1 kg load was used as a workpiece. The workpiece surface was ground and polished to Sa around 0.09 µm prior to the scratching tests. Diameter of the steel wheel was measured as 34.8 mm and a run-out error was less than 1 µm. CBN grit was glued onto the circumferential surface of the steel wheel by using Loctite super glue. The workpiece surface was tilted slightly to allow scratches with different depth of cuts. Peripheral cutting speed during scratching was 327.6 m/min. More about description of the scratching process and scratching method can be found in detail in reference (Öpöz and Chen, 2012).

The scratch profile of the samples were measured by using Talysurf CCI 3000 interferometer. A view of 3D profile measurement is shown in Figure 1- (b). After 3D profiles of the scratches were obtained, 2D cross sectional profiles were extracted at every 3.23 µm increment along the scratch length in order to measure the depth of groove, groove area and pile-up area. In the context of this paper, material removal along the scratch path for a single scratch was investigated and compared with FEM simulation. Prominent material removal mechanism is decided using a measure of pile up ratio, which is defined as the ratio of total pile up area to total groove section area in the cross section. The pile up area and groove section area were calculated by using Mountains software (TalyMap universal version 3.1.9).

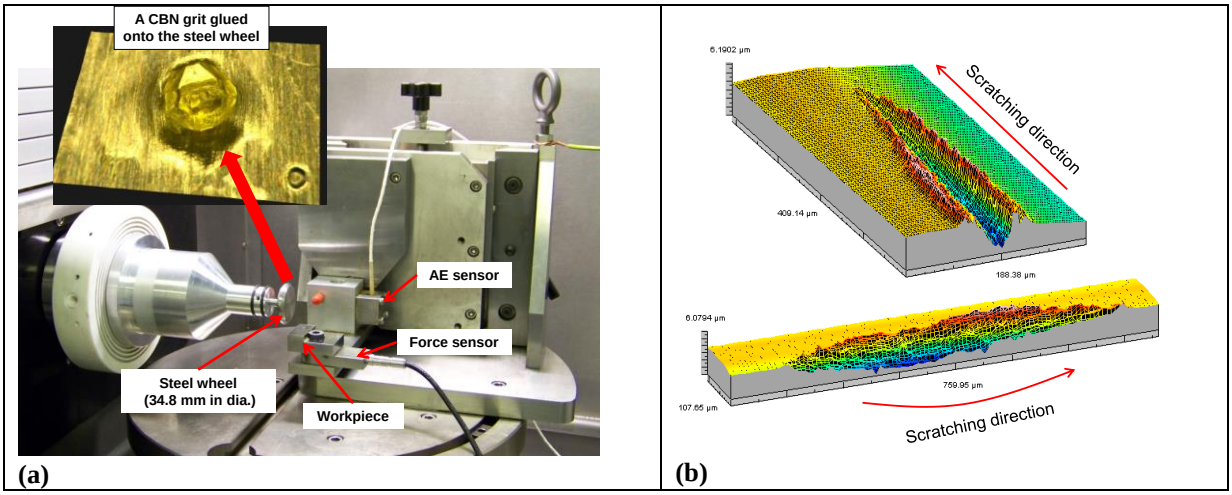

Figure 1: (a) Single grit scratching test setup and (b) 3D cross sectional views of a scratch.

3 FINITE ELEMENT MODELLING

Simplified model of scratch simulations were performed in Abaqus/Standard. Grit simulation path used during simulation is shown in Figure 2-(a). It consist of five steps. Grit speed is not considered and simulation step time is 1 sec for each step, so simulations were performed at very slow speed (100 µm/s horizontal velocity). The workpiece material properties(similar to mild steel) is given in Table 1. Grit was modelled using CBN material properties with Young's modulus E=909 GPa, Poisson's ratio ν=0.121, and density ρ=3400 kg.m^{-3}, in the shape of a half-spherical solid with a radius 100 µm. Remeshing was applied to the workpiece to reduce the element size and increase scratch profile accuracy (Öpöz and Chen, 2011). Element size in the workpiece contact region is less than 1 µm while element size in the grit body is around 4 µm. The grit-workpiece model is shown in Figure 2-(b). Friction coefficients of zero and 0.2 were used to investigate the effect on ploughing mechanism. Total number of elements used in the simulation is 184085. Approximate CPU time for each simulation is 48 hours using a computer with an Intel(R) core(TM) i7 CPU 960 @ 3.20 GHz and 12 GB of RAM.

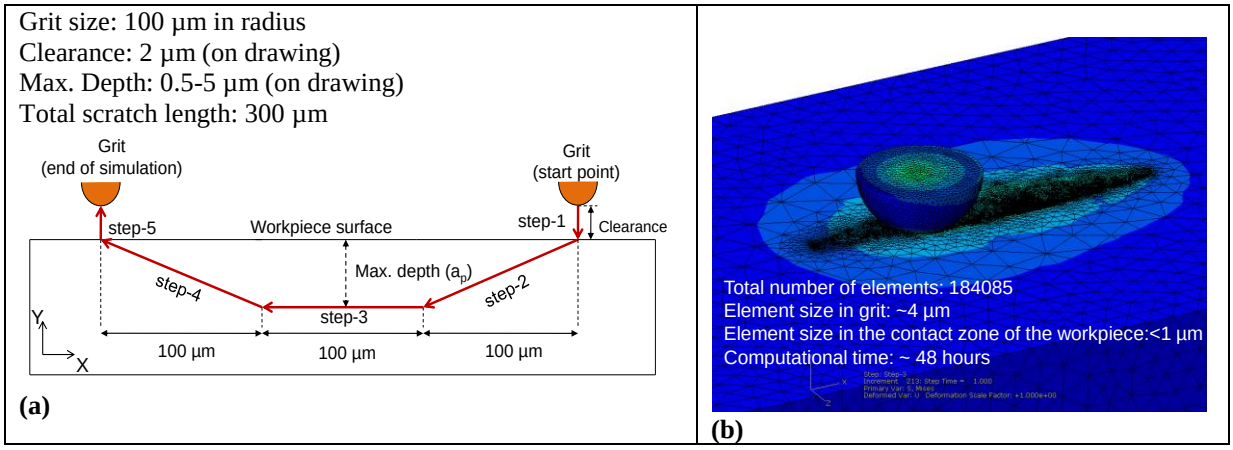

Figure 2: (a) Grit simulation path and (b) FEM model.

Table 1: Material properties used in FEM simulations (similar to mild steel, but smaller yield stress and plastic strain to make deformation more clear).

Mass density (kg/ m^3)	7800
Young's modulus (GPa)	200
Poisson's ratio ν	0.3
Yield stress σ (MPa)	Plastic strain ε_p (mm/mm)
180	0
200	0.1
250	0.25
300	0.3

4 RESULTS

4.1 Experimental Results

The pile-up ratio variation along the single scratch is shown in Figure 3, where the point with high cutting efficiency can be found by looking at the lowest pile-up ratio along the scratch length. At the initial stage of grit-workpiece interaction, pile-ratio was found relatively high around 1~3, that shows at that region no cutting occur and only material swelling up due to plastic deformation. Before the ploughing stage, rubbing action may occur but cannot be observed. Pile-up ratio gradually decreases while scratch depth increases towards the deepest point of the scratch. When the scratch depth decreases, the pile-up ratio increases again until the grit-workpiece interaction finishes. While grit is moving towards the end of scratch path, the grit pushes ploughed material forward and some portion of this material could flow along the two sides of the scratch. Therefore, it is apparent in Figure 3 that the pile-up ratio at the exit side of scratch becomes very high even to the range of 10 to 30. Cutting become more efficient with increasing of depth of cut. However, at similar depths of cut, higher pile up ratio was obtained at the exit side of the scratch compared to the entrance side of the scratch. So, it can be inferred that cutting efficiency was decreasing rapidly towards the end of scratch, while it was increasing fast at the beginning of scratch until reaching maximum depth.

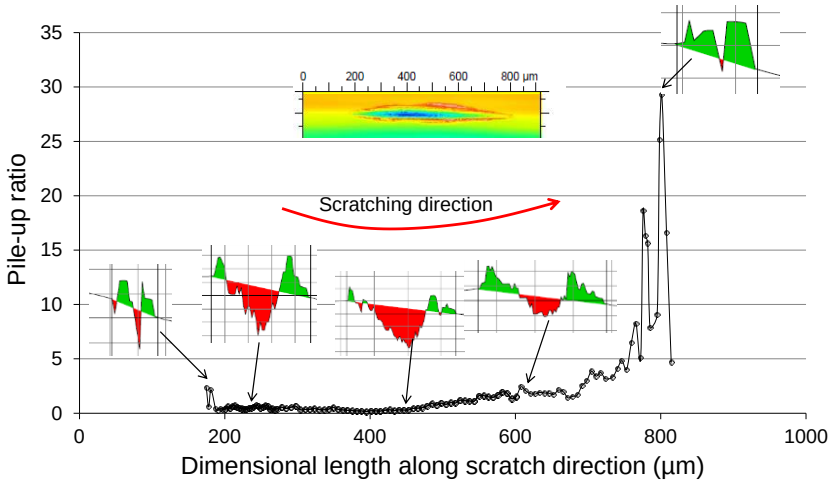

Figure 3: Pile up ratio along scratch length

4.2 Finite Element Simulations

Figure 4 shows the deformation due to grit frictionless scratching with maximum depth of 5 µm. Figure 4 (top picture) shows elastic and plastic deformation during grit-workpiece engagement when the grit was at the end of step-3. At this point, the total deformation in vertical direction including elastic and plastic components is around 5.36 µm, but total deformation at the same location after grit

was moved to the end of the simulation path is around 4.1 µm. The difference of 1.16 µm can attribute to elastic deformation. Figure 5 shows some cross sectional profiles from the approximate location of the middle of step-2, end of step-2, end of step-3 and the middle of step-4 together with calculated pile up and groove area. Figure 6 shows the variations in pile-up ratio along the single grit simulation path. Pile-up ratios gradually increase along step-3 due to material accumulation with the grit advancement. As a result, the deeper the depth of cut, the higher the pile up ratio as seen in Figure 6. However in step-4 there is a dramatic increase in pile-up ratio. This is because the grit climbs up to the end of the scratch simulation. This shows that the ploughing mechanism is completely different in the grit entrance and grit exit during grinding. Simulation results are strongly supported by the single grit scratch tests; see Figure 3. From the observations in the middle of step-4 (at position of 250 µm in Figure 6) pile-up ratio increases with increase in maximum depth. In addition, pile-up ratio is also affected by the friction coefficient. It is clear from Figure 6, higher pile-up ratio is obtained with friction.

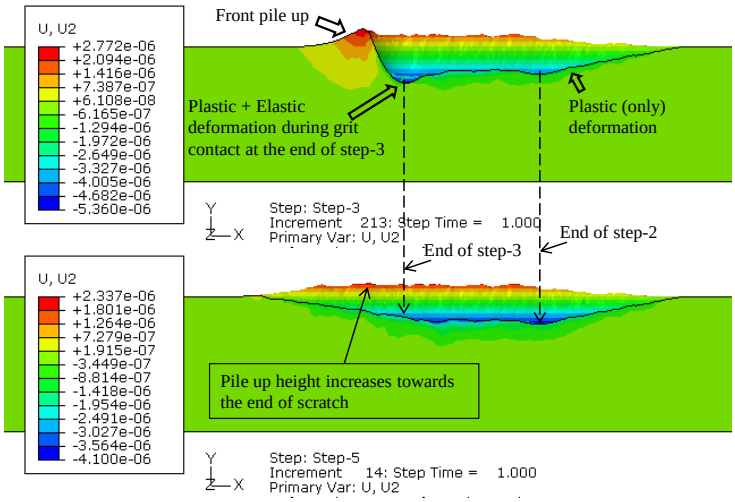

Figure 4: Simulation transactional view along scratching path.

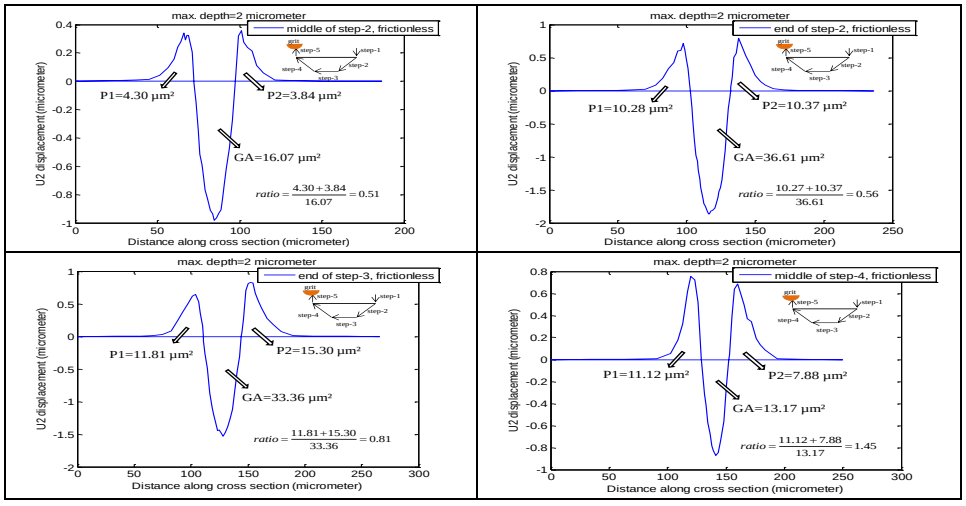

Figure 5: Cross sectional profiles at different location along the scratch path.

5 CONCLUSIONS

Both experiments and FEM simulations support each other in terms of material flow and material removal during the grit scratching. Pile up ratio was proved to be a good measure to illustrate material removal mechanism changes along the scratching direction. It was found that the pile up ratio continuously increases towards the end of scratch after grit passed its deepest cutting depth. At the

exit part of the scratch, very high pile up ratios present and the scratch surface could be above the original surface, which indicates no material removal anymore but the grit may leave ploughed materials on the workpiece surface. Friction contributes to ploughing effect positively. Consequently, cutting is more effective at the entrance side of the scratch until the maximum cutting depth, then becomes less effective dramatically towards the end of scratch. These results will help understanding the differences of material removal mechanisms in the upcut and downcut grinding.

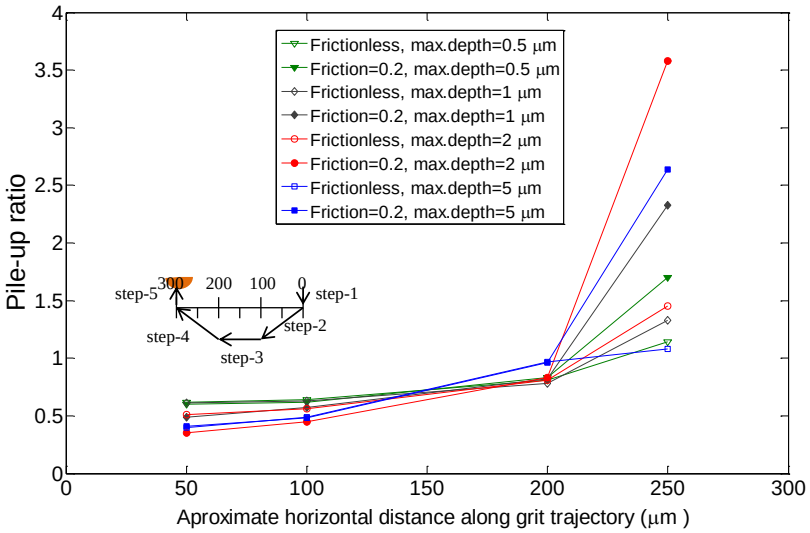

Figure 6: Pile up ratio along the scratch path.

REFERENCES

Anderson, D., A. Warkentin, R. Bauer. 2011. Experimental and numerical investigations of single abrasive-grain cutting. *International Journal of Machine Tools and Manufacture* 51: 898-910.

Doman, D.A., A. Warkentin, R. Bauer. 2009b. Experimentally validated finite element model of the rubbing and ploughing phases in scratch tests. *Proceedings of the Institution of Mechanical Engineers, Part B: Journal of Engineering Manufacture* 223: 1519-1527.

Ghosh, S., A.B. Chattopadhyay, S. Paul. 2008. Modelling of specific energy requirement during high-efficiency deep grinding. *International Journal of Machine Tools and Manufacture* 48: 1242-1253.

Hahn, R.S. 1962. On the nature of the grinding process. In *Proceedings of the 3rd International Machine Tool Design & Research Conference*, Manchester, 129-154.

Komanduri, R. 1971. Some aspects of machining with negative rake tools simulating grinding. *International Journal of Machine Tool Design and Research* 11: 223-233.

König, W., K. Steffens, T. Ludewig. 1985. Single grit tests to reveal the fundamental mechanism in grinding. In *Milton C. Shaw (Ed.) Grinding Symposium*, Miami Beach, FL, 141-154.

Klocke, F., T. Beck, S. Hoppe, T. Krieg, N. Müller, T. Nöthe, H-W. Raedt, K. Sweeney. 2002. Examples of FEM application in manufacturing technology. *Journal of Materials Processing Technology* 120: 450-457.

Öpöz, T.T., X. Chen. 2011. Single Grit Grinding Simulation by Using Finite Element Analysis. In *American Institute of Physics Conference Proceeding* 1315: 1467-1472.

Öpöz, T.T., X. Chen. 2012. Experimental investigation of material removal mechanism in single grit grinding. *International Journal of Machine Tools and Manufacture* 63: 32-40.

Rowe, W. B., X. Chen. 1997. Characterisation of the Size Effect in Grinding and the Sliced Bread Analogy. *The International Journal of Production Research* 35: 887-899.

Takenaka, N. 1966. A study on the grinding action by single grit. *Ann. CIRP* 13: 183-190.

Wang, H., G. Subhash, A. Chandra. 2001. Characteristics of single-grit rotating scratch with a conical tool on pure titanium. *Wear* 249: 566-581.